

SKN-1 links *C. elegans* mesendodermal specification to a conserved oxidative stress response

Jae Hyung An and T. Keith Blackwell¹

Center for Blood Research and Department of Pathology, Harvard Medical School, Boston, Massachusetts 02115, USA

During the earliest stages of *Caenorhabditis elegans* embryogenesis, the transcription factor SKN-1 initiates development of the digestive system and other mesendodermal tissues. Postembryonic SKN-1 functions have not been elucidated. SKN-1 binds to DNA through a unique mechanism, but is distantly related to basic leucine-zipper proteins that orchestrate the major oxidative stress response in vertebrates and yeast. Here we show that despite its distinct mode of target gene recognition, SKN-1 functions similarly to resist oxidative stress in *C. elegans*. During postembryonic stages, SKN-1 regulates a key Phase II detoxification gene through constitutive and stress-inducible mechanisms in the ASI chemosensory neurons and intestine, respectively. SKN-1 is present in ASI nuclei under normal conditions, and accumulates in intestinal nuclei in response to oxidative stress. *skn-1* mutants are sensitive to oxidative stress and have shortened lifespans. SKN-1 represents a connection between developmental specification of the digestive system and one of its most basic functions, resistance to oxidative and xenobiotic stress. This oxidative stress response thus appears to be both widely conserved and ancient, suggesting that the mesendodermal specification role of SKN-1 was predated by its function in these detoxification mechanisms.

[**Keywords:** Oxidative stress; *C. elegans*; SKN-1; mesendoderm; intestine; lifespan]

Received April 29, 2003; revised version accepted June 6, 2003.

In diverse organisms, a common mesendodermal tissue field gives rise to the endoderm and a mesoderm subset that forms the heart and blood in vertebrates (Reiter et al. 1999; Warga and Nusslein-Volhard 1999; Rodaway and Patient 2001). In the nematode *Caenorhabditis elegans*, mesendodermal development is initiated by the transcription factor SKN-1, which was identified in a screen for genes that are required maternally for formation of pharyngeal tissue (Bowerman et al. 1992). Maternally expressed SKN-1 specifies the fate of a single cell, the EMS blastomere (Fig. 1A). The EMS daughter cell E becomes the endoderm, which consists of the intestine. Its sister cell MS gives rise to mesodermal derivatives that include the posterior portion of the pharynx, a feeding pump that is analogous to the heart, and coelomocytes that resemble macrophages. The anterior pharynx is specified in ABa descendants by a SKN-1-dependent signal from MS. In *skn-1* mutants, these lineages instead give rise to excess hypodermis (Bowerman et al. 1992).

SKN-1 directly induces expression of the GATA factors MED-1 and MED-2, which are required for mesendodermal differentiation in the EMS lineage (Fig. 1A;

Maduro et al. 2001). Remarkably, counterparts of the MED proteins (GATA4, GATA5, and GATA6) and of various downstream transcription factors involved in *C. elegans* mesendodermal development appear to play surprisingly similar roles in vertebrates (Haun et al. 1998; Reiter et al. 1999; Shoichet et al. 2000; Rodaway and Patient 2001; Lickert et al. 2002; Maduro and Rothman 2002). These similarities suggest that certain key regulatory mechanisms involved in mesendodermal differentiation have been maintained during evolution.

Although many aspects of mesendodermal development appear to be conserved, it is striking that SKN-1 is distinct from any other known protein because of its DNA-binding mechanism. SKN-1 binds to DNA with high affinity as a monomer through a basic region (BR) like those of basic leucine-zipper (bZIP) proteins, which are obligate dimers (Fig. 1B; Blackwell et al. 1994). SKN-1 lacks a ZIP segment, which is essential for bZIP protein DNA binding because it acts as a dimerization element, and stabilizes folding of the BR on the DNA (Talanian et al. 1990). In contrast, monomeric SKN-1 DNA binding is comparably stabilized by a flexible "arm" that binds in the minor groove, and by a novel variant of the CNC region, through which SKN-1 is distantly related to a bZIP protein subgroup (Blackwell et al. 1994; Carroll et al. 1997; Kophengnavong et al. 1999). SKN-1 is also similar to two vertebrate CNC-group proteins (NF-E2-related

¹Corresponding author.

E-MAIL blackwell@cbr.med.harvard.edu; FAX (617) 278-3153.

Article published online ahead of print. Article and publication date are at <http://www.genesdev.org/cgi/doi/10.1101/gad.1107803>.

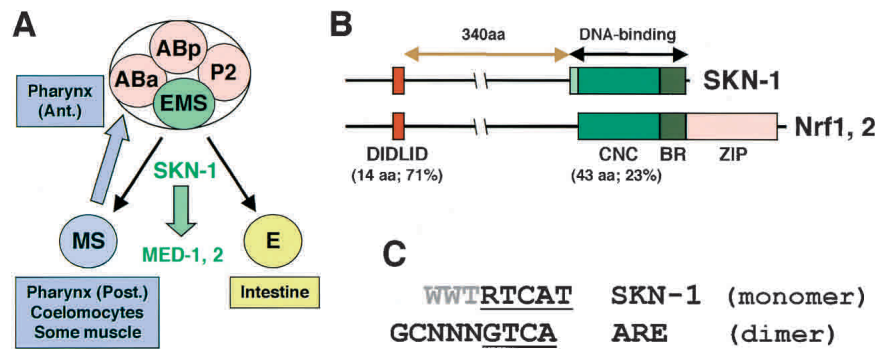


Figure 1. SKN-1 embryonic functions and comparison to Nrf proteins. (A) Cell fate specification. In four-cell embryos, SKN-1 initiates mesodermal development by establishing the EMS blastomere fate (Bowerman et al. 1992). Anterior is to the left, and ventral at the bottom. (B) SKN-1 compared to Nrf proteins. The SKN-1 minor groove-binding arm is shown in light green. The percent identity between SKN-1 and mouse Nrf2 regions is indicated. (C) Consensus sequences for SKN-1 binding and the ARE. The SKN-1 BR recognizes a consensus bZIP half-site

(underlined) adjacent to an AT-rich motif (gray) that is specified by the arm (B). Nrf proteins bind to the ARE as obligate heterodimers with Maf or other bZIP proteins (Hayes and McMahon 2001). (R) G/A; (W) T/A.

factors Nrf1 and Nrf2) within a 14-amino-acid transactivator element (DIDLID; Fig. 1B; Walker et al. 2000). These limited similarities suggest that although SKN-1-like proteins have not been identified outside of nematodes, SKN-1 and these particular bZIP proteins might share a common precursor.

In vertebrates, Nrf proteins activate transcription of genes encoding the Phase II detoxification enzymes, which constitute the primary cellular defense against oxidative stress (Hayes and McMahon 2001; Thimmulappa et al. 2002). Essentially all organisms must defend themselves against reactive oxygen species (ROS), which are derived from both mitochondrial respiration and exogenous sources. Phase II enzymes synthesize the critical reducing agent glutathione, scavenge ROS directly, and detoxify reactive intermediates that are generated when xenobiotics are metabolized by the cytochrome p450 (Phase I) enzymes. Through Nrf2, exposure to oxidative stress or particular classes of chemicals induces Phase II enzyme gene expression in a variety of tissues, including the liver and digestive tract (Itoh et al. 1997; Hayes and McMahon 2001; Wolf 2001). This mechanism also constitutes the major response to chemoprotective antioxidants, including many natural compounds, which thereby stimulate xenobiotic detoxification and inhibit carcinogen-induced tumorigenesis. Accordingly, mice that lack *Nrf2* are abnormally susceptible to drug toxicity and carcinogenesis, and do not respond to chemoprotective antioxidants (Chan and Kan 1999; Chan et al. 2001; Ramos-Gomez et al. 2001; Fahey et al. 2002).

Nrf-related bZIP proteins regulate Phase II genes in *Saccharomyces cerevisiae* (Yap1p) and *Schizosaccharomyces pombe* (Pap1p; Toone et al. 2001), suggesting that this ROS response may be generally conserved among eukaryotes. It has therefore been perplexing that bZIP orthologs of these proteins are not present in *C. elegans*. One possibility is that *C. elegans* has developed different mechanisms of regulating Phase II detoxification genes. Alternatively, the limited similarities between SKN-1 and Nrf proteins raise the surprising possibility that despite its unique DNA-binding mechanism, SKN-1 might be functionally related to Nrf proteins. *skn-1* has post-embryonic functions that have not been characterized: although homozygotes of all *skn-1* alleles are viable and

fertile, heterozygotes between *skn-1* and a corresponding deficiency (*nDf41*) usually die with abnormal intestines (Bowerman et al. 1992). Although this suggests that existing *skn-1* alleles might not be true nulls, it also indicates that *skn-1* has functions in the differentiated intestine.

Here we have determined that during postembryonic stages, SKN-1 functions similarly to Nrf proteins in responses to oxidative stress, and that *skn-1* is required for oxidative stress resistance and longevity. Expression of a key ROS-resistance gene is regulated independently of *skn-1* in some *C. elegans* tissues, however, indicating that metazoans customize oxidative stress defenses for different organ contexts. The oxidative stress response mediated by SKN-1 appears to be conserved among *C. elegans*, vertebrates, and single-celled eukaryotes, implying that this is an ancient pathway, and that the role of SKN-1 in initiating mesodermal development may have arisen from this detoxification mechanism.

Results

Constitutive and inducible Phase II detoxification gene activation by SKN-1

Vertebrate Nrf proteins induce expression of Phase II detoxification enzyme genes by binding to the characteristic antioxidant response element (ARE) in their promoters (Fig. 1C; Hayes and McMahon 2001). We have searched for SKN-1-binding sites within the predicted promoters of *C. elegans* orthologs of these oxidative-stress-resistance genes. The SKN-1-binding site preference and the ARE are distinct but not mutually exclusive (Fig. 1C). A predicted SKN-1 site should appear randomly every 2048 bp, but between two and four SKN-1 sites are present within 1 kb upstream of multiple *C. elegans* genes that encode predicted Phase II detoxification enzymes, including γ -glutamyl cysteine synthetase heavy chain [GCS(h)], glutathione synthetase, and four glutathione S-transferase (GST) isoforms (Table 1). In vertebrates, each of these genes is activated by Nrf proteins (Hayes and McMahon 2001). SKN-1 sites or variants that differ at only one AT-rich region position are similarly present 5' of the Nrf target *NADH quinone*

Table 1. Predicted SKN-1-binding sites upstream of *C. elegans* oxidative stress-resistance genes

Enzymes	Gene or ORF	Location ^a	Direction	Sequence
γ -Glutamyl-cysteine synthetase heavy chain (GCS(h))	<i>gcs-1</i>	-121	→	TTTATCAT
		-316	←	ATGACTTA
		-607	←	ATGACAAT
Glutathione synthetase	M176.2	-137	→	TTTGTCAT
		-169	←	ATGACAAA
		-243	→	TTTATCAT
		-378	←	ATGATTTT
NADH quinone oxidoreductase	F39B2.3	-469	→	GTTATCAT
Glutathione S-transferase	R03D7.6	-518	←	ATGACAAT
		-149	←	ATGACAAT
		-282	←	ATGATTTT
		-302	←	ATGACATT
		-947	←	ATGATTTT
	F35E8.8	-94	←	ATGACAAT
		-240	←	ATGATAAT
	F11G11.2	-133	←	ATGACAAA
		-391	→	CTTATCAT
	K08F4.7	-83	←	ATGACATT
-157		→	TTTGTCAT	
Superoxide dismutase	<i>sod-1</i>	-64	→	ATAATCAT
		-191	→	TGTATCAT
	<i>sod-2</i>	-363	←	ATGACAAT
		-959	→	AGAATCAT
		-980	→	AGAATCAT
Catalase	<i>sod-3</i>	-287	→	TAAATCAT
		-880	→	ATGATCAT
	<i>ctl-1</i>	-978	→	GTCATCAT
		-997	→	CTTATCAT

The SKN-1-binding consensus is shown in Figure 1C.

^aThe A within the translation initiation codon is designated as base 1.

oxidoreductase, the catalase *ctl-1*, and superoxide dismutases (*sod-1*, *sod-2*, and *sod-3*; Table 1).

The presence of SKN-1 site clusters upstream of multiple *C. elegans* Phase II detoxification genes is consistent with SKN-1 functioning analogously to Nrf proteins. To test this hypothesis, we investigated whether SKN-1 is required to express the Phase II gene *gcs-1* (Table 1). *gcs-1* is the *C. elegans* ortholog of *GCS(h)*, a representative and well-characterized Nrf-protein target gene that in yeast is regulated by Yap1p and Pap1p (Toone and Jones 1999; Hayes and McMahon 2001). The GCS(h) enzyme is important for oxidative stress resistance because it is rate-limiting for glutathione synthesis.

We investigated *gcs-1* expression in *C. elegans* using a transgene that included the predicted *gcs-1* promoter, along with the 17 N-terminal GCS-1 amino acids fused to green fluorescent protein (GFP). This promoter segment contained three consensus SKN-1-binding sites, and corresponded to the intervening sequence between *gcs-1* and the nearest upstream gene (data not shown). With this strategy, we could analyze *gcs-1* expression independently of GCS-1 protein stability. In a wild-type background, during larval and adult stages GCS-1::GFP was readily detectable in the pharynx, and in nearby cells that appeared to be neurons (Fig. 2A,B). By soaking *gcs-1::gfp* lines in DiI, a dye that fills amphid sensory neu-

rons (Herman and Hedgecock 1990), we determined that two GCS-1::GFP-expressing cells located adjacent to the posterior pharynx correspond to the ASI chemosensory neurons (Fig. 2C,D), which prevent constitutive entry into the dauer diapause state (Ren et al. 1996; Schackwitz et al. 1996). GCS-1::GFP expression was also apparent anteriorly and posteriorly in the intestine (Fig. 2A,B).

In vertebrates, oxidative stress induces Phase II gene expression through an Nrf2-dependent pathway in the intestine and liver (Itoh et al. 1997; Hayes and McMahon 2001). Similarly, stimuli that cause oxidative stress dramatically increased GCS-1::GFP expression in the *C. elegans* intestine (Fig. 2E,F; Table 2). This response was triggered by both heat and the herbicide paraquat (methyl viologen), which generates intracellular superoxide anions. To investigate the involvement of *skn-1* in *gcs-1* expression, we introduced the *gcs-1::gfp* transgene into the *skn-1(zu67)* background, the *skn-1* allele that is associated with the most severe embryonic phenotype (Bowerman et al. 1992). Under both normal and oxidative stress conditions, in *skn-1(zu67)* homozygotes GCS-1::GFP was apparent at wild-type levels in the pharynx, but was otherwise undetectable (Fig. 2G–L), indicating that *skn-1* is essential for both constitutive and inducible *gcs-1::gfp* expression outside of the pharynx.

Promoter mutagenesis identified discrete elements that are required for these *skn-1*-dependent and -inde-

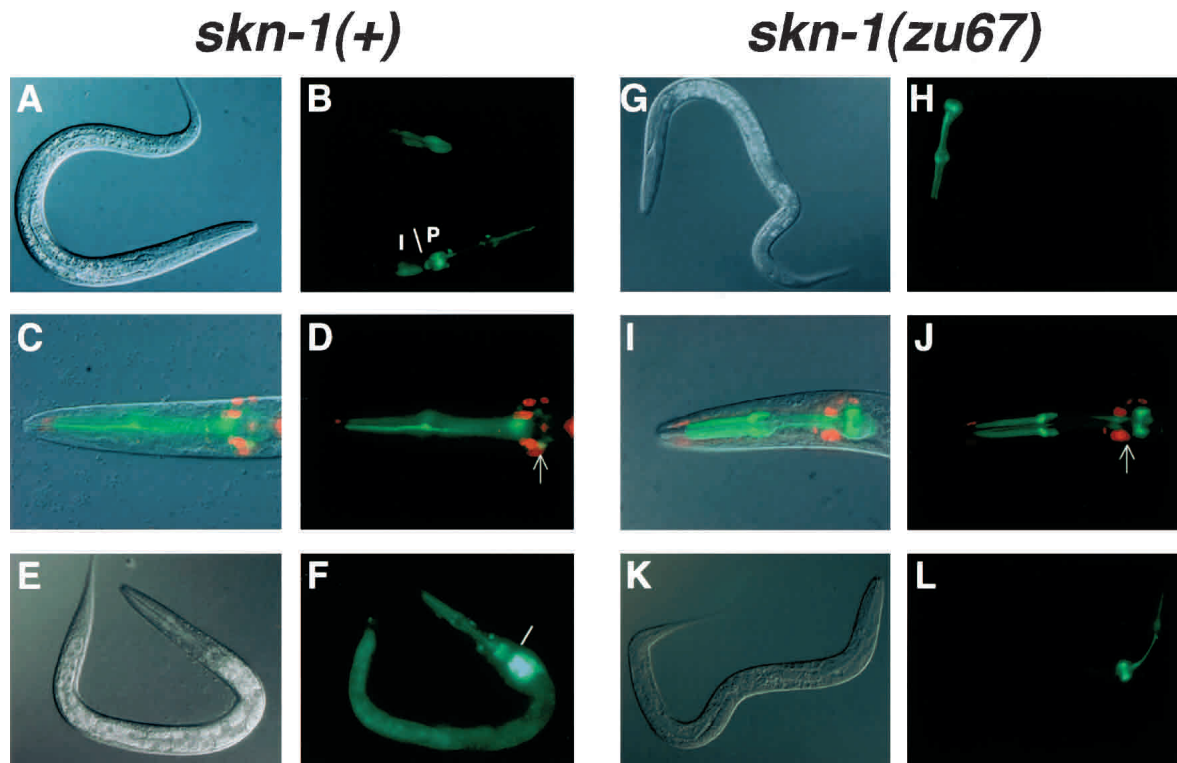


Figure 2. *skn-1*-dependent GCS-1::GFP expression in the intestine and ASI neurons. (A–F) GCS-1::GFP expression in wild-type animals. A *gcs-1* genomic fragment containing its 17 N-terminal codons and 1840 upstream base pairs was fused to the N terminus of GFP, which contained a nuclear localization signal. The expression patterns shown are each representative of more than two independent transgenic lines, and of all postembryonic stages examined (L2–adult; data not shown). (A,B) Nomarski (A) and fluorescent (B) views of an L2 larva. (B) A line demarcates the approximate boundary between the anterior intestine (I) and posterior pharynx (P). (C,D) Combined Nomarski/fluorescent (C) and fluorescent (D) views of the head of a typical L4-stage animal that had been exposed to DiI. (D) One of the two ASI neurons is indicated with an arrow. (E,F) An L2 larva in which GCS-1::GFP expression was induced to high levels in the intestine by heat. A similar induction occurred in response to paraquat (Table 2). The boundary between the anterior intestine and posterior pharynx is indicated as in B. (G–L) GCS-1::GFP was not detectable outside of the pharynx in *skn-1* homozygotes. Typical animals are shown from experiments that parallel those displayed to the left in A–F. Note the absence of GCS-1::GFP in the intestine and ASI neurons under normal conditions (G–J), and after treatment with heat (K,L) or paraquat (data not shown). In two independent transgenic lines, in a homozygous *skn-1* background GCS-1::GFP expression was not detected in these tissues in any animals under either normal or induction conditions.

pendent *gcs-1* expression patterns. Pharyngeal GCS-1::GFP expression was abolished by removal of the distal *gcs-1* promoter region (*gcsΔ2::gfp*; Fig. 3A,B), which lacks SKN-1-binding sites but contains consensus sites

for the pharyngeal transcription factors PEB-1 and PHA-4 (Thatcher et al. 2001; Gaudet and Mango 2002; data not shown). The remaining proximal 682 bp of the *gcs-1* promoter included the three predicted SKN-1-binding sites,

Table 2. Induction of GCS-1::GFP expression in the intestine by oxidative stress

Inducer	<i>gcs-1::gfp</i>				<i>gcsΔ2::gfp</i>			
	Low	Medium	High	N	Low	Medium	High	N
Control	90.8%	7.9%	1.3%	76	88.2%	10.3%	1.5%	68
Heat shock	10.5%	72.4%	17.1%	76	0.0%	14.0%	86.0%	86
paraquat	14.5%	67.1%	18.4%	76	21.3%	65.6%	13.1%	61

A representative set of experiments involving a mixed population of L2–young adult worms is shown, from which the percentages of animals in each expression category are listed. Induction of GCS-1::GFP expression was comparable among the different developmental stages analyzed. “Low” refers to animals similar to that in Figure 2A, in which intestinal GCS-1::GFP was apparent at modest levels anteriorly, or anteriorly and posteriorly. “High” indicates that GCS-1::GFP was present at high levels anteriorly and detectable throughout most of the intestine, as in Figure 2F. “Medium” refers to animals in which GCS-1::GFP was present at high levels anteriorly as in Figure 2F and possibly posteriorly, but was not detected in between. N indicates the number of animals analyzed from each transgenic strain.

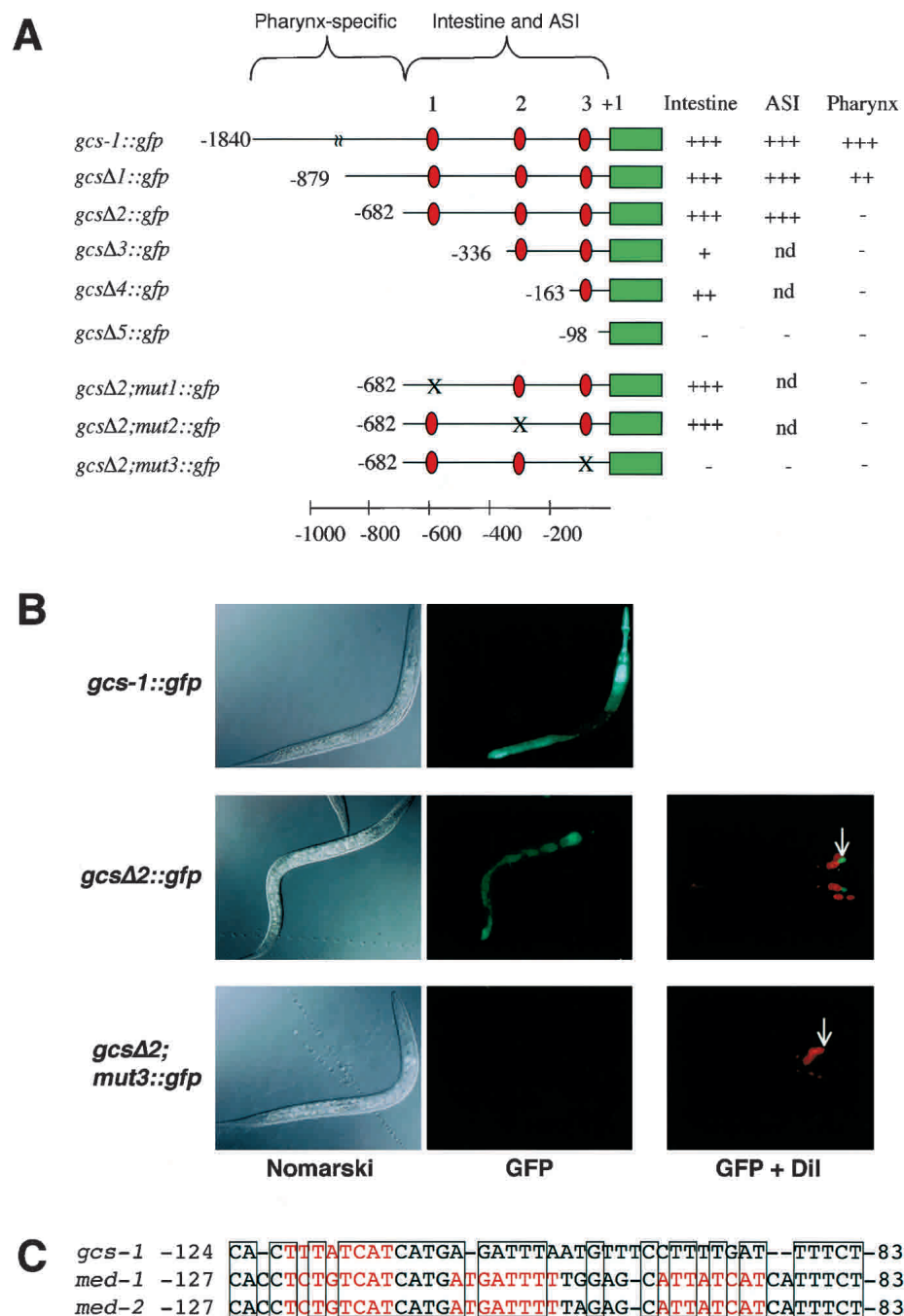


Figure 3. Specific elements required for *skn-1*-independent and -dependent GCS-1::GFP expression. (A) Analysis of the *gcs-1* promoter. The expression of the indicated constructs from transgenic extrachromosomal arrays was assayed in two to three independent transgenic lines under normal conditions, and after induction by paraquat and heat. The relative expression levels in the tissues designated to the *right* (data not shown) are indicated by plus signs, with ++ indicating a reproducible reduction and + indicating barely detectable expression. Within each set of transgenic lines that carried promoter mutations, levels of normal and induced expression were affected in parallel. Mutations that were created in predicted SKN-1 sites 1, 2, and 3 are described in Materials and Methods, and are not compatible with SKN-1 binding (Blackwell et al. 1994; see text). Red ovals indicate predicted SKN-1 binding sites and a green bar indicates the 5'-end of the *gcs-1::gfp* coding region. Map numbers refer to the predicted translation start. (B) Uncoupling pharyngeal GCS-1::GFP expression from intestinal and ASI neuron expression. The *gcsΔ2* mutation eliminated pharyngeal GCS-1::GFP expression, but allowed near-wild-type levels of ASI and intestinal expression. Concurrent ablation of SKN-1 binding site 3 (*gcsΔ2, mut3*) eliminated transgene expression in all tissues. Paraquat-treated worms are shown in the GFP column. (C) Composite *gcs-1* promoter element that includes SKN-1 site 3, and is also present in the *med-1* and *med-2* promoters. SKN-1 binding sites are red, and identical sequences are boxed.

and was sufficient for appropriate GCS-1::GFP expression in the intestine and ASI neurons (*gcsΔ2::gfp*; Fig. 3A,B; Table 2). Constitutive and stress-induced GCS-1::GFP expression within the intestine and ASI neurons did not require SKN-1-binding sites 1 or 2 individually, but was abolished by alteration of site 3 (*gcsΔ2*; *mut3::gfp*; Fig. 3A,B; see Materials and Methods).

Remarkably, SKN-1-binding site 3 is located within a 42-bp *gcs-1* promoter element that is similar to a composite motif through which SKN-1 activates *med-1* and *med-2* in the embryo (Figs. 1A, 3C; Maduro et al. 2001). The conservation between these *gcs-1* and *med* promoter elements is particularly striking because they are located at identical distances from their respective translation starts, but contain different numbers of SKN-1 sites (Fig. 3C). In an electrophoretic mobility shift assay (EMSA), full-length SKN-1 and the 85-amino-acid SKN-1 DNA-binding domain (SKN Domain; Blackwell et al. 1994) each bound sequence-specifically to SKN-1-binding site 3 in the context of this *gcs-1* promoter element (Fig. 4). These SKN-1 proteins bound with high affinity to an oligonucleotide that corresponds to this composite element (wild type; Fig. 4A,B, lanes 2–5), but not to an

analogous probe in which SKN-1 site 3 had been altered as in the inactive *gcsΔ2*; *mut3::gfp* transgene (Fig. 3A; mutant, Fig. 4A,B, lanes 7–10). Binding of these SKN-1 proteins to the wild-type probe was also competed much more effectively by unlabeled wild-type than mutant DNA (Fig. 4A,B, lanes 11–20). Further supporting the importance of this *gcs-1* promoter element, a 163-bp fragment that includes it provides significant GCS-1::GFP expression in the intestine, but 5' truncation within this sequence inactivates the promoter (*gcsΔ4::gfp* and *gcsΔ5::gfp*; Fig. 3A). In addition, an apparent counterpart to SKN-1 site 3 is present within 200 bp of the translation start site of the *Caenorhabditis briggsae gcs-1* gene (data not shown). We conclude that binding of SKN-1 to site 3 is required for *gcs-1* expression in the intestine and ASI neurons.

SKN-1 expression and accumulation in intestinal nuclei in response to oxidative stress

Postembryonic expression of SKN-1 has not been investigated previously. To determine whether SKN-1 is present in tissues where it is required for *gcs-1::gfp* expression, we analyzed expression of a transgene in which GFP is fused to the C terminus of full-length SKN-1 (SKN-1::GFP; Fig. 5A). Although maternal *skn-1::gfp* expression was not readily detectable because of germline transgene silencing (Kelly et al. 1997), at a low frequency this transgene rescued the embryonic defect in *skn-1(zu67)* homozygotes (data not shown), indicating that this SKN-1::GFP fusion protein is functional.

In the embryo, antibody staining previously revealed the presence of maternal SKN-1 in nuclei through the eight-cell stage, then detected zygotically expressed SKN-1 in only ~15% of late-stage embryos that had ceased dividing (Bowerman et al. 1993). We uniformly detected nuclear SKN-1::GFP in intestinal precursors beginning at the 50–100-cell stage (Fig. 5B), then in both the intestine and hypodermis (Fig. 5C), indicating that SKN-1 is expressed zygotically earlier than it is detectable by antibody staining. In late-stage embryos, SKN-1::GFP was also present in intestinal nuclei but not in the hypodermis (Fig. 5D), suggesting that hypodermal *skn-1* expression may be maintained by a region located outside of this transgene.

In contrast to the embryo, in larvae and young adults, SKN-1::GFP was usually present at very low levels in intestinal nuclei (Fig. 5F; Table 3). SKN-1::GFP was readily detectable in the ASI neurons, where *gcs-1::gfp* was constitutively expressed (Fig. 5E,F), but not in other cells in the head, where GCS-1::GFP expression appeared to be *skn-1*-dependent (Fig. 2B,H). The latter *skn-1* dependence might be indirect, or derived from low-level SKN-1 expression or distant *skn-1* regulatory regions. The finding that SKN-1::GFP is present at only modest levels in intestinal nuclei raises the question of how oxidative stress induces *skn-1*-dependent intestinal *gcs-1* expression (Figs. 2, 3; Table 2). In cultured mammalian cells, Nrf2 is stabilized and relocalized from the cytoplasm to the nucleus in response to oxidative stress

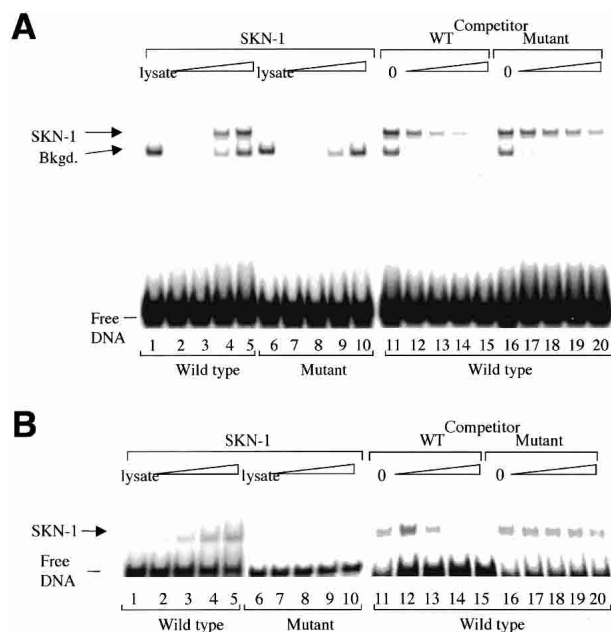


Figure 4. Specific binding of SKN-1 to an essential *gcs-1* promoter sequence. (A) Binding of full-length SKN-1 to site 3 within the *gcs-1* composite element, assayed by EMSA. (Lanes 2–5) Binding of increasing amounts of in vitro translated SKN-1 protein (0, 0.25, 0.5, and 3 μ L translation lysate; indicated by a triangle) to the wild-type site. (Lane 1) Binding to 3 μ L of unprogrammed lysate. A background species is labeled. (Lanes 6–10) The same assay performed with the mutant probe. (Lanes 11–20) SKN-1 DNA binding is assayed in the presence of the indicated unlabeled competitor oligonucleotides. Lanes 12–15 and 17–20 correspond to addition of a 20-, 50-, 150-, and 400-fold molar excess of competitor over the labeled wild-type DNA. (B) The in vitro translated SKN-1 DNA-binding domain (Fig. 1B) binds specifically to the *gcs-1* composite element. Binding was assayed as in A.

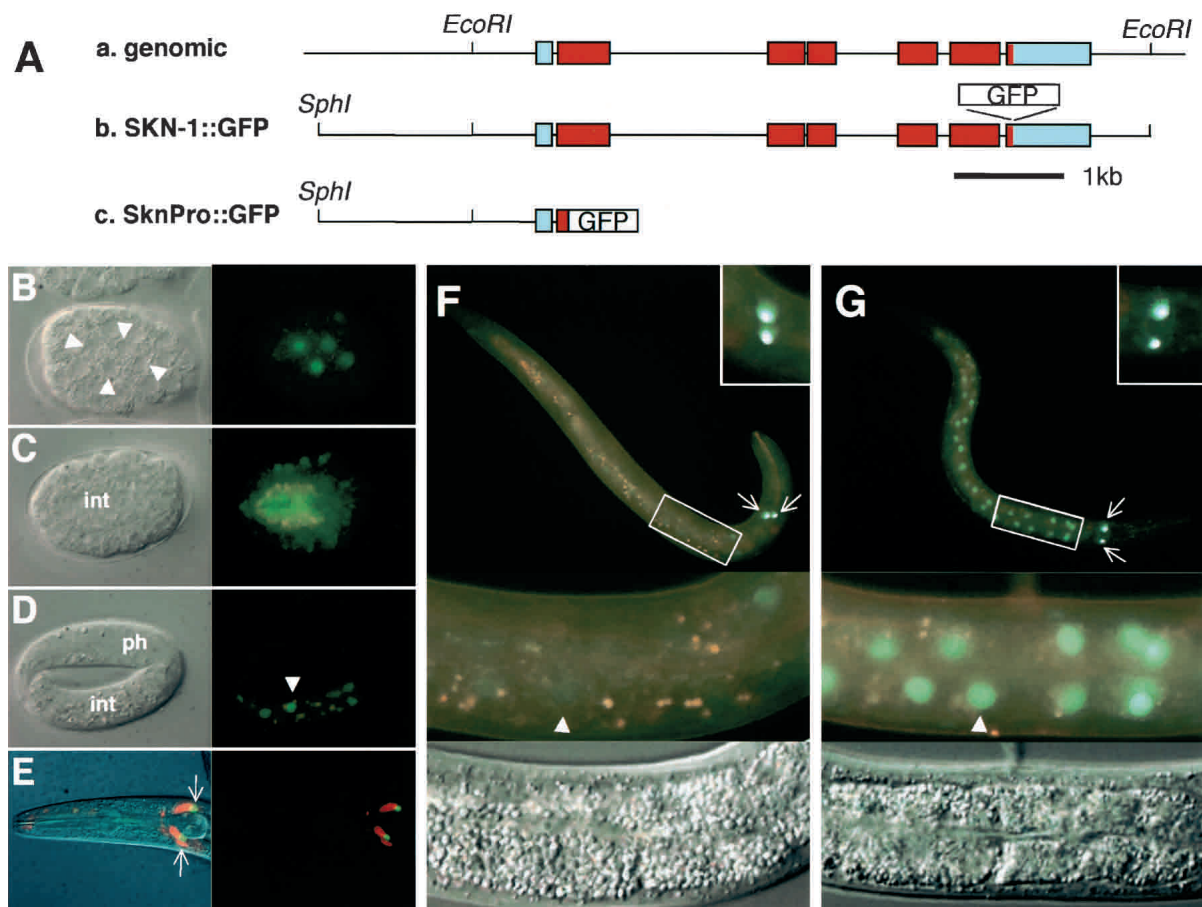


Figure 5. Expression and stress-induced nuclear accumulation of SKN-1::GFP. (A) SKN-1::GFP transgenes. (a) *skn-1* gene. Transcribed coding and untranslated regions are indicated in red and blue, respectively. (b) SKN-1::GFP translational fusion construct, which includes an *EcoRI* fragment that previously rescued maternal *skn-1* lethality (Bowerman et al. 1992). *C. elegans* DNA is indicated by a black line. (c) SknPro::GFP promoter fusion, in which the 38 N-terminal SKN-1 amino acids are fused to GFP containing a nuclear localization signal. (B–D) Embryonic expression of SKN-1::GFP. Nomarski (left) and fluorescent (right) views of 100-cell (B), 280-min (C), and threefold (D) embryos. Endogenous intestinal autofluorescence is visible as yellow or orange (see Materials and Methods). White triangles, intestine precursor nuclei; int, intestine; ph, pharynx. (E) SKN-1::GFP expression in ASI neurons (arrows). Nomarski/fluorescent (left) and fluorescent (right) views are shown of a typical DiI-exposed L4 larva. (F) Larval SKN-1::GFP expression under normal conditions. (Bottom) Fluorescent and Nomarski closeups of the boxed central region of this L2. An intestinal nucleus is indicated by a white triangle, and the ASI neurons (arrows) are shown in detail in the top right box. (G) SKN-1::GFP localization under oxidative stress. A heat-shocked L2 is shown, but similar results were obtained after exposure to other oxidative stress inducers (Table 3). The integrated strain *Is007* is shown, but two extrachromosomal lines and a different integrated line exhibited similar patterns.

(Itoh et al. 1999; Sekhar et al. 2002; Nguyen et al. 2003; Stewart et al. 2003). A promoter fusion transgene in which only the SKN-1 N terminus was linked to GFP (SknPro::GFP; Fig. 5A) was constitutively expressed at high levels in all intestinal cells (data not shown), suggesting that SKN-1 expression or localization might also be regulated posttranscriptionally by oxidative stress.

After exposure to either paraquat or heat, neither the location nor intensity of SKN-1::GFP was detectably altered in the ASI neurons, but in a high percentage of animals, elevated levels of SKN-1::GFP appeared in intestinal cell nuclei, particularly anteriorly and posteriorly, where GCS-1::GFP is most robustly expressed (Fig. 5F,G; Table 3). SKN-1::GFP accumulated in intestinal nuclei within 5 min after treatment with 50 mM sodium azide (Table 3),

which induces oxidative stress by blocking mitochondrial electron transport. The rapidity of this last response indicates that SKN-1 is constitutively present in the intestine but may be diffuse within the cytoplasm and masked by autofluorescence. This accumulation of SKN-1::GFP in intestinal nuclei in response to oxidative stress remarkably parallels the *skn-1*-dependent induction of GCS-1::GFP under similar conditions, supporting the model that SKN-1 activates intestinal *gcs-1* expression directly.

skn-1 required for oxidative stress resistance and normal longevity

The functional similarities between SKN-1 and Nrf proteins that we have identified predict that *skn-1* mutants

Table 3. Accumulation of SKN-1::GFP in intestinal nuclei in response to oxidative stress

Inducer	Low	Medium	High	N
Control	78.9%	14.5%	6.6%	76
Heat	5.6%	11.9%	82.5%	143
Paraquat	53.1%	43.8%	3.1%	64
M9, 5 min	74.7%	17.6%	7.7%	91
50 mM sodium azide, 5 min	0.8%	44.2%	55.0%	120

Mixed-stage L2-young adult transgenic worms were exposed to the indicated conditions. A representative set of experiments is shown, from which the percentages of animals in each category are listed. SKN-1 localization patterns did not differ significantly among the different developmental stages examined. M9 refers to the control incubation for the sodium azide experiment. In some animals treated with sodium azide, high levels of nuclear SKN-1::GFP appeared in <1 min (data not shown). "Low" refers to animals in which SKN-1::GFP was barely detectable in all intestinal nuclei, as shown in Figure 4F. "High" indicates that a very strong SKN-1::GFP signal was present in all intestinal nuclei, as in Figure 4G. "Medium" refers to animals in which nuclear SKN-1::GFP was present at high levels anteriorly or anteriorly and posteriorly, but was barely detectable midway through the intestine. N indicates the number of animals analyzed in each category.

may be abnormally sensitive to oxidative stress. *skn-1(zu67)* homozygotes produce normal numbers of offspring with normal timing, and as young adults are not obviously distinguishable in morphology from wild type (data not shown). Two different *skn-1* mutant alleles are associated with markedly decreased survival in the presence of paraquat, however, indicating that *skn-1* mutants are sensitive to oxidative stress (Fig. 6A).

Numerous correlations between oxidative stress resistance and longevity have been described (Finkel and Holbrook 2000; Finch and Ruvkun 2001; Dillin et al. 2002; Hekimi and Guarente 2003; Holzenberger et al. 2003). Administration of superoxide dismutase mimetics increases *C. elegans* lifespan by ~40% (Melov et al. 2000). Insulin/IGF-1-like signaling reduces *C. elegans* lifespan by inhibiting the Foxo-type transcription factor DAF-16, which promotes longevity in part by increasing expression of ROS-resistance genes (Kenyon et al. 1993; Honda and Honda 1999; Finch and Ruvkun 2001; Henderson and Johnson 2001; Lee et al. 2003). Given these precedents, we examined whether *skn-1* homozygotes live as long as wild type. Both the mean and maximum lifespans of *skn-1(zu67)* and *skn-1(zu129)* homozygotes were reduced by 25%–30% (Fig. 6B; Table 4), indicating that SKN-1 is required for normal longevity.

Discussion

A conserved postembryonic function for SKN-1 in oxidative stress resistance

We have determined that the *C. elegans* developmental specification protein SKN-1 also mediates a conserved response to oxidative stress. SKN-1 functions similarly to bZIP proteins that regulate Phase II detoxification

genes in vertebrates (Nrf1, Nrf2) and yeast (Yap1p, Pap1p). SKN-1 activates a conserved Phase II gene in the intestine and ASI neurons (Figs. 2, 3, 5), SKN-1-binding sites flank *C. elegans* orthologs of additional Nrf target genes (Table 1), and *skn-1* mutants are sensitive to oxidative stress (Fig. 6A). The accumulation of SKN-1 in intestinal nuclei in response to oxidative stress (Fig. 5G; Table 3) may parallel nuclear accumulation of Nrf proteins, Yap1p, and Pap1p, under these conditions (Itoh et al. 1999; Toone et al. 2001; Delaunay et al. 2002). It is possible that the intestinal abnormalities in *skn-1(zu67)/nDf41* larvae (Bowerman et al. 1992) involve oxidative stress, because 10%–20% of *gcs-1(RNAi)* animals also die as larvae with abnormal intestines (data not shown).

These parallels between SKN-1 and Nrf proteins are surprising because the mechanism through which SKN-1 binds DNA is both unique and highly divergent (Blackwell et al. 1994). SKN-1 and Nrf proteins are most similar within the 14-amino-acid DIDLID transactivation element (Fig. 1B; Walker et al. 2000), which appears to be present only in SKN-1 and Nrf protein orthologs, suggesting that in metazoans, preservation of this ele-

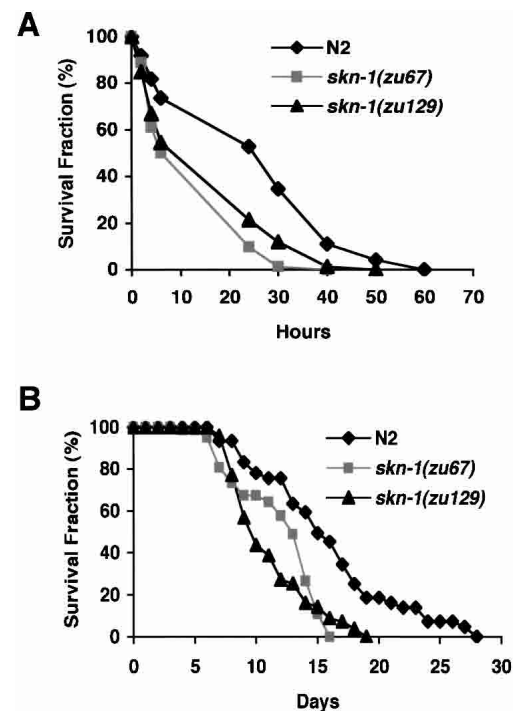


Figure 6. *skn-1* mutants are sensitive to oxidative stress and have reduced lifespans. (A) Paraquat sensitivity. Individual worms were scored for survival at the times shown after they had been placed in M9 that contained 100 mM paraquat. An average of three experiments involving 24 worms each is graphed. Among these experiments, for *skn-1(zu67)* and *skn-1(zu129)* animals, the mean survival times expressed as percentage of wild type were $52.9\% \pm 9.5\%$ and $60.7\% \pm 16.1\%$, respectively. All wild-type and *skn-1* mutant worms survived a parallel control 72-h incubation in M9 alone (data not shown). (B) Lifespan assay. Worms were maintained at 20°C and scored for survival at the indicated time after the L4 stage. An average of three consecutive experiments involving 25–28 worms each is plotted (Table 4).

Table 4. *Reduced lifespan of skn-1 mutants*

Genotype	Mean lifespan \pm SD (days) (% wild-type)	Maximum lifespan (days) (% wild-type)	Mean maximum lifespan \pm SD (days) (% wild-type)
Wild type (N2)	15.9 \pm 2.2 (100)	28 (100)	24.3 \pm 3.5 (100)
<i>skn-1(zu67)</i>	11.8 \pm 1.4 (74)	17 (61)	16.3 \pm 0.6 (67)
<i>skn-1(zu129)</i>	11.1 \pm 0.1 (70)	19 (68)	18.7 \pm 0.6 (77)

Lifespan data are taken from the three experiments that are averaged in the plot shown in Figure 6B. Maximum lifespan refers to the longest lifespan observed in any of the three experiments. Mean maximum lifespan refers to the mean among the maxima for these experiments. S.D., standard deviation.

ment has been of critical importance for this oxidative stress response. It will now be of interest to determine whether an uncharacterized *C. elegans* gene that is closely related to *skn-1* (Bowerman et al. 1993) might also be involved in oxidative stress resistance. Here we have studied the originally described *skn-1* gene, which rescues the maternal *skn-1* defect (Bowerman et al. 1992). In addition to this full-length SKN-1 species, sequence databases predict the existence of two other SKN-1 forms. One of these includes 90 additional N-terminal residues, and the other consists primarily of the 234 C-terminal SKN-1 residues (data not shown). It will be interesting to determine whether these SKN-1 forms respond to oxidative stress. Our findings also raise the intriguing question of whether Nrf proteins and SKN-1 might have similar developmental functions. *Nrf2*^{-/-} mice are viable, but *Nrf1* knockouts caused either an erythroid defect, or abnormal gastrulation and lack of mesoderm (Farmer et al. 1997; Itoh et al. 1997; Chan et al. 1998). The latter phenotype is reminiscent of the maternal *skn-1* defect. To determine whether *Nrf1* and *Nrf2* have redundant developmental functions, it will be necessary to disrupt these genes simultaneously.

Although *gcs-1* expression in the intestine is induced by SKN-1 in response to stress, the presence of nuclear SKN-1 allows *gcs-1* to be expressed constitutively in the ASI neurons, and *gcs-1* expression is *skn-1*-independent in the pharynx (Fig. 2). In metazoans, Phase II genes thus can be activated through distinct pathways that may be important for functions of different tissues. For example, the finding that *skn-1* functions constitutively in the ASI neurons, which inhibit dauer entry, suggests that although *skn-1(zu67)* homozygotes can enter the dauer stage (data not shown), *skn-1* or oxidative stress might influence regulation of this process.

The lifespan reduction that we observed in *skn-1* mutants (25%–30%; Fig. 6B; Table 4) is comparable to that reported in *daf-16* mutants (20%; Kenyon et al. 1993; Lee et al. 2001). In *C. elegans*, aging involves pleiotropic changes that vary among individuals, and mutations that influence lifespan may affect aging of some tissues more than others (Garigan et al. 2002; Herndon et al. 2002). Just before death, the anterior intestine and posterior pharynx degenerated more frequently in *skn-1* animals than wild type (data not shown), a finding that may reflect aging but does not exclude the possibility of an additional defect. At 1 wk after hatching, small cavities and apparent yolk droplets appeared in the heads of

many *skn-1* but not wild-type animals (data not shown). These changes are typical of aging *C. elegans* (Garigan et al. 2002; Herndon et al. 2002), suggesting that *skn-1* mutants may age prematurely. Some mechanisms that regulate *C. elegans* lifespan have been shown to influence lifespan in higher metazoans (Clancy et al. 2001; Finch and Ruvkun 2001; Bluher et al. 2003; Holzenberger et al. 2003). The observation that normal *C. elegans* longevity requires *skn-1* is consistent with other associations between oxidative stress resistance and lifespan (see Results), and suggests that the conserved oxidative-stress-resistance pathway regulated by SKN-1 might influence longevity in other species.

Oxidative stress contributes to human pathologies that include diabetes, atherosclerosis, neurodegenerative diseases, reperfusion injury, and HIV infection (Finkel and Holbrook 2000; Droge 2002). The ROS defenses mobilized by human Nrf proteins are thought to be beneficial in those diverse disease states. This gene activation pathway is also important for drug detoxification, and therefore for chemotherapeutic agent tolerance, and it may provide a widely applicable means of cancer prevention (Chan et al. 2001; Hayes and McMahon 2001; Wolf 2001). For example, dietary consumption of chemoprotective antioxidants acts through Nrf2 to inhibit chemical carcinogenesis in mice, and decreases the risk of gastrointestinal and lung tumors in humans (Ramos-Gomez et al. 2001; Fahey et al. 2002; Thimmulappa et al. 2002). The functional parallels between SKN-1 and Nrf proteins indicate that it may be possible to derive novel therapeutic modalities and targets by investigating this detoxification system in *C. elegans*, a metazoan that is highly amenable to genetic and pharmacologic screening.

Mesendoderm specification by an oxidative stress response factor

It is striking that SKN-1 initiates embryonic development of the mesendoderm, then is critical for one of the most basic functions of endodermal organs, ROS detoxification. Some organs are induced to develop by transcription factors that later regulate downstream differentiation genes (Gehring and Ikeo 1999; Gaudet and Mango 2002). SKN-1 represents an extreme example of a connection between development and function because it initiates formation of multiple organs, including the entire feeding and digestive system. The remarkable functional conservation among SKN-1, Nrf proteins, and

their yeast counterparts suggest that this oxidative stress response function of SKN-1 is ancient, and presumably predates its developmental role in mesoderm specification. The digestive system handles energy intake and processing, and responses to external stresses. Mesodermal tissues that are developmentally linked to the endoderm, the *C. elegans* pharynx and the vertebrate heart and hematopoietic system, are also involved in nutrient intake and transfer and responses to exogenous agents. SKN-1 may have been co-opted for a fate specification role after these organs evolved. On the other hand, the mesoderm itself might have arisen as a tissue set that was functionally linked to these ancestral detoxification mechanisms.

Materials and methods

C. elegans strains and bioinformatics

Strains were maintained at 20°C unless otherwise noted, using standard methods (Brenner 1974). The alleles used were N2 Bristol as the wild type, and *skn-1(zu67)* and *skn-1(zu129)* (Bowerman et al. 1992). *C. elegans* orthologs of Nrf targets and other detoxification genes were identified by searching WORMpep or genomic databases (Sanger Centre). Predicted SKN-1 sites (Fig. 1C) 5' of their coding regions were identified with TFSEARCH (Heinemeyer et al. 1998).

Paraquat sensitivity and lifespan assays

To assay sensitivity to paraquat, young adults were transferred from NGM agar plates into 24-well plates (6 per well) containing 0.3 μ L of M9 that either did or did not contain 100 mM paraquat. Worms were incubated at 20°C, and the number of dead animals was counted by the continuous absence of swimming movements and pharyngeal pumping. Lifespan assays were performed essentially as described by Hsin and Kenyon (1999). Animals were transferred to new plates daily and classified as dead when they did not move after repeated prodding with a pick. Animals that crawled away from the plate, exploded, or contained internally hatched worms were excluded from the analysis.

Plasmid constructions

All PCR was performed using Pfu polymerase (Stratagene). GFP vectors pPD95.67 and pPD114.35 were gifts from Andrew Fire (Carnegie Institute of Washington, Baltimore, MD). We created an *skn-1::gfp* promoter fusion construct (SknPro::GFP; Fig. 5A) by ligating GFP vector pPD95.67 and a PCR-amplified 2.1-kb clone containing the promoter region and 38 amino acids from the first ATG codon of the *skn-1* gene from cosmid T19E7. To generate the SKN-1::GFP translational fusion construct (Fig. 5A), the 5.7-kb *EcoRI* DNA fragment that rescues the maternal *skn-1* phenotype and encodes the 533-amino-acid SKN-1 protein (Bowerman et al. 1992) was amplified from cosmid B0547. A *ClaI* site was created immediately 3' to the SKN-1 C terminus by the QuikChange method (Stratagene), which was used for all site-directed mutagenesis. This *EcoRI* fragment was subcloned into pUC18, which contained the upstream 1.3-kb *SphI-EcoRI* fragment from SknPro::GFP (Fig. 5A). A 0.8-kb *ClaI* fragment that contained the GFP open reading frame (amplified from plasmid pPD114.35) was then cloned into the *ClaI* site to generate an in-frame exon fusion of GFP to the SKN-1 C terminus.

The *C. elegans gcs-1* ORF (F37B12.2) is between 45% and 54% identical to human, mouse, *Drosophila*, and yeast GCS(h) (data not shown). To construct the *gcs-1::gfp* transgene, a fragment that contained 1840 bp upstream of the initiation ATG, along with sequences encoding the 17 N-terminal GCS-1 residues, was amplified by PCR from cosmid F37B12, and cloned into GFP vector pPD95.67. Promoter deletions were similarly constructed by PCR. In *gcs-1* point mutation constructs, predicted SKN-1 sites (underlined) were altered as follows: Site 1, -608 GATGACAAT to CTGCAGAAT; Site 2, -317 GATGACTTA to CTGCAGTTA; and Site 3, -121 TTTATCATC to TTTCTGCAG.

Transgenic analyses

Transgenic strains were generated by injecting DNA into the gonad of young adult animals as described (Mello et al. 1991). *gcs-1::gfp* transgene constructs (Fig. 3A) were injected at 50 ng/ μ L along with the *rol-6* marker (pRF4) at 100 ng/ μ L. Between three and six independent extrachromosomal lines were generated and analyzed for each *gcs-1::gfp* construct. To investigate GCS-1::GFP expression in the *skn-1(zu67)* background, *rol-6*-marked *gcs-1::gfp* hermaphrodites were mated with N2 males; then their transgenic progeny were crossed with *skn-1(zu67)/DnT1* hermaphrodites, which have an *unc* phenotype. After transgenic males were successively crossed twice with *skn-1(zu67)/DnT1* hermaphrodites, *unc; rol F3* hermaphrodite progeny were selected. From this population, *skn-1(zu67)/DnT1; gcs-1::gfp* animals were identified on the basis of their non-*unc; rol* progeny laying dead eggs. Two different *gcs-1::gfp* lines were thereby crossed into the *skn-1(zu67)* background and examined for GFP expression. DIC and fluorescence images were acquired with a Zeiss AxioSKOP2 microscope and AxioCam cooled color digital camera.

To investigate expression of *gcs-1::gfp* and mutant transgenes, worms were exposed to oxidative stress under the following conditions. For heat shock, worms cultured at 20°C were transferred onto prewarmed seeded plates and incubated at 29°C for 20 h, then examined by fluorescence microscopy for GFP expression. *gcs-1::gfp* induction was also observed in an alternative heat treatment protocol, during which worms cultured at 20°C were transferred onto prewarmed plates and incubated at 34°C for 2–4 h, then returned to 20°C and examined for GFP expression hourly during a 4-h recovery period. In the experiments described in Table 2, young adults were transferred to plates that contained 1 mM paraquat in the agar and maintained at 20°C for 3 d prior to analysis. In an alternative induction protocol, worms that carried *gcs-1::gfp* or the mutant transgenes shown in Figure 3A were incubated in M9 either with or without 100 mM paraquat for 30 min, then allowed to recover on plates for 4 h. The latter procedure also resulted in induction of intestinal *gcs-1::gfp* expression by paraquat but was associated with a higher background in uninduced animals.

To create transgenic *skn-1::gfp* strains, 2.5, 10, or 50 ng/ μ L of transgene DNA (Fig. 5A) was injected into N2 animals along with 100 ng/ μ L of pRF4 to generate extrachromosomal transgenic lines. Two different extrachromosomal arrays, *Ex001* and *Ex007*, generated with 2.5 and 10 ng/ μ L of SKN-1::GFP, respectively, were integrated into the chromosome by UV irradiation (400 J/m²) to produce the insertion strains *Is001* and *Is007*, respectively. To rescue the embryonic lethality of an *skn-1* mutation, SKN-1::GFP was injected into *skn-1(zu67)/DnT1* animals at 2.5 ng/ μ L with 100 ng/ μ L of the pRF4 marker. Rescue of maternal *skn-1* lethality was observed in some *rol; non-unc* progeny but not in non-*rol; non-unc* animals.

SKN-1::GFP expression analyses shown were performed in

the *Is007* strain, but essentially the same results were obtained in analyses of *Ex001*, *Ex007*, and *Is001* (data not shown). To analyze expression and localization of SKN-1::GFP in response to oxidative stress, *skn-1::gfp* transgenic worms were treated as described above for the *gcs-1::gfp* expression studies. In addition, for exposure to sodium azide, animals cultured at 20°C were placed on a 2% agarose pad on a slide in M9 either with or without 50 mM sodium azide, then covered with a slip and examined by fluorescence microscopy. These worms were scored for the presence of SKN-1::GFP in intestinal nuclei 5 min later. For photography, worms were immobilized with either 2 mM sodium azide (Figs. 2, 3) or 2 mM levamisole (Fig. 5). These treatments did not stimulate either GCS-1::GFP induction or SKN-1::GFP relocation during the times examined (data not shown). No immobilization agent was used in the experiments shown in Tables 2 and 3. To discriminate intestinal autofluorescence from SKN-1::GFP epifluorescence, a triple-band emission filter set (Chroma 61000) was used in conjunction with a narrow-band excitation filter (484/14 nm). This combination allowed autofluorescence to be detected as yellow/orange fluorescence deriving from a combined green and red signal, while GFP remained green.

Worms that carried *skn-1::gfp*, *gcs-1::gfp*, and *gcs-1::gfp* mutant transgenes were incubated with 50 µg/mL DiI (Molecular Probes) in M9 at 20°C for 3 h, then transferred to fresh plates for 1 h to destain, and examined under the fluorescence microscope. The ASI chemosensory neurons were identified by according to their intensity of DiI labeling and location relative to other DiI-labeled cells.

DNA-binding assays

Full-length SKN-1 and the SKN domain were expressed by *in vitro* translation (Promega) as described previously (Carroll et al. 1997). Oligonucleotide probes were end-labeled using Klenow and α -³²P-labeled dATP and CTP, then purified using QIAquick Kit (QIAGEN). EMSAs were performed essentially as described in (Blackwell et al. 1994), with labeled probes present at 2.5×10^{-9} M.

Acknowledgments

We thank Bruce Bowerman, Grace Gill, Yang Shi, Siu Sylvia Lee, Kaveh Ashrafi, Elizabeth Veal, and Blackwell lab members for helpful discussions, technical advice, or critical reading of this manuscript. For reagents we thank Andrew Fire, Alan Coulson, Yuji Kohara, and the *Caenorhabditis* genetics center. We thank Courtney DiPaolo for technical assistance, and are particularly grateful to Amy Walker for contributions to early stages of this project. This work was supported by a grant from the NIH to T.K.B. (GM62891).

The publication costs of this article were defrayed in part by payment of page charges. This article must therefore be hereby marked "advertisement" in accordance with 18 USC section 1734 solely to indicate this fact.

References

- Blackwell, T.K., Bowerman, B., Priess, J., and Weintraub, H. 1994. Formation of a monomeric DNA binding domain by Skn-1 bZIP and homeodomain elements. *Science* **266**: 621–628.
- Bluher, M., Kahn, B.B., and Kahn, C.R. 2003. Extended longevity in mice lacking the insulin receptor in adipose tissue. *Science* **299**: 572–574.
- Bowerman, B., Eaton, B.A., and Priess, J.R. 1992. *skn-1*, a maternally expressed gene required to specify the fate of ventral blastomeres in the early *C. elegans* embryo. *Cell* **68**: 1061–1075.
- Bowerman, B., Draper, B.W., Mello, C., and Priess, J. 1993. The maternal gene *skn-1* encodes a protein that is distributed unequally in early *C. elegans* embryos. *Cell* **74**: 443–452.
- Brenner, S. 1974. The genetics of *Caenorhabditis elegans*. *Genetics* **77**: 71–94.
- Carroll, A.S., Gilbert, D.E., Liu, X., Cheung, J.W., Michnowicz, J.E., Wagner, G., Ellenberger, T.E., and Blackwell, T.K. 1997. SKN-1 domain folding and basic region monomer stabilization upon DNA binding. *Genes & Dev.* **11**: 2227–2238.
- Chan, J.Y., Kwong, M., Lu, R., Chang, J., Wang, B., Yen, T.S., and Kan, Y.W. 1998. Targeted disruption of the ubiquitous CNC-bZIP transcription factor, Nrf-1, results in anemia and embryonic lethality in mice. *EMBO J.* **17**: 1779–1787.
- Chan, K. and Kan, Y.W. 1999. Nrf2 is essential for protection against acute pulmonary injury in mice. *Proc. Natl. Acad. Sci.* **96**: 12731–12736.
- Chan, K., Han, X.D., and Kan, Y.W. 2001. An important function of Nrf2 in combating oxidative stress: Detoxification of acetaminophen. *Proc. Natl. Acad. Sci.* **98**: 4611–4616.
- Clancy, D.J., Gems, D., Harshman, L.G., Oldham, S., Stocker, H., Hafen, E., Leivers, S.J., and Partridge, L. 2001. Extension of life-span by loss of CHICO, a *Drosophila* insulin receptor substrate protein. *Science* **292**: 104–106.
- Delaunay, A., Pflieger, D., Barrault, M.B., Vinh, J., and Tolodano, M.B. 2002. A thiol peroxidase is an H₂O₂ receptor and redox-transducer in gene activation. *Cell* **111**: 471–481.
- Dillin, A., Crawford, D.K., and Kenyon, C. 2002. Timing requirements for insulin/IGF-1 signaling in *C. elegans*. *Science* **298**: 830–834.
- Droge, W. 2002. Free radicals in the physiological control of cell function. *Physiol. Rev.* **82**: 47–95.
- Fahey, J.W., Haristoy, X., Dolan, P.M., Kensler, T.W., Scholtus, I., Stephenson, K.K., Talalay, P., and Lozniewski, A. 2002. Sulforaphane inhibits extracellular, intracellular, and antibiotic-resistant strains of *Helicobacter pylori* and prevents benzo[a]pyrene-induced stomach tumors. *Proc. Natl. Acad. Sci.* **99**: 7610–7615.
- Farmer, S.C., Sun, C.W., Winnier, G.E., Hogan, B.L., and Townes, T.M. 1997. The bZIP transcription factor LCR-F1 is essential for mesoderm formation in mouse development. *Genes & Dev.* **11**: 786–798.
- Finch, C.E. and Ruvkun, G. 2001. The genetics of aging. *Annu. Rev. Genomics Hum. Genet.* **2**: 435–462.
- Finkel, T. and Holbrook, N.J. 2000. Oxidants, oxidative stress and the biology of ageing. *Nature* **408**: 239–247.
- Garigan, D., Hsu, A.L., Fraser, A.G., Kamath, R.S., Ahringer, J., and Kenyon, C. 2002. Genetic analysis of tissue aging in *Caenorhabditis elegans*. A role for heat-shock factor and bacterial proliferation. *Genetics* **161**: 1101–1112.
- Gaudet, J. and Mango, S.E. 2002. Regulation of organogenesis by the *Caenorhabditis elegans* FoxA protein PHA-4. *Science* **295**: 821–825.
- Gehring, W.J. and Ikeo, K. 1999. Pax 6: Mastering eye morphogenesis and eye evolution. *Trends Genet.* **15**: 371–377.
- Haun, C., Alexander, J., Stainier, D.Y., and Okkema, P.G. 1998. Rescue of *Caenorhabditis elegans* pharyngeal development by a vertebrate heart specification gene. *Proc. Natl. Acad. Sci.* **95**: 5072–5075.
- Hayes, J.D. and McMahon, M. 2001. Molecular basis for the contribution of the antioxidant responsive element to cancer chemoprevention. *Cancer Lett.* **174**: 103–113.
- Heinemeyer, T., Wingender, E., Reuter, I., Hermjakob, H., Kel, A.E., Kel, O.V., Ignatieva, E.V., Ananko, E.A., Podkolodnaya, O.A., Kolpakov, F.A., et al. 1998. Databases on transcriptional regulation: TRANSFAC, TRRD and COMPEL. *Nucleic Acids Res.* **26**: 362–367.

- Hekimi, S. and Guarente, L. 2003. Genetics and the specificity of the aging process. *Science* **299**: 1351–1354.
- Henderson, S.T. and Johnson, T.E. 2001. *daf-16* integrates developmental and environmental inputs to mediate aging in the nematode *Caenorhabditis elegans*. *Curr. Biol.* **11**: 1975–1980.
- Herman, R.K. and Hedgecock, E.M. 1990. Limitation of the size of the vulval primordium of *Caenorhabditis elegans* by *lin-15* expression in surrounding hypodermis. *Nature* **348**: 169–171.
- Herndon, L.A., Schmeissner, P.J., Dudaronek, J.M., Brown, P.A., Listner, K.M., Sakano, Y., Paupard, M.C., Hall, D.H., and Driscoll, M. 2002. Stochastic and genetic factors influence tissue-specific decline in ageing *C. elegans*. *Nature* **419**: 808–814.
- Holzenberger, M., Dupont, J., Ducos, B., Leneuve, P., Geloën, A., Even, P.C., Cervera, P., and Le Bouc, Y. 2003. IGF-1 receptor regulates lifespan and resistance to oxidative stress in mice. *Nature* **421**: 182–187.
- Honda, Y. and Honda, S. 1999. The *daf-2* gene network for longevity regulates oxidative stress resistance and Mn-superoxide dismutase gene expression in *Caenorhabditis elegans*. *FASEB J.* **13**: 1385–1393.
- Hsin, H. and Kenyon, C. 1999. Signals from the reproductive system regulate the lifespan of *C. elegans*. *Nature* **399**: 362–366.
- Itoh, K., Chiba, T., Takahashi, S., Ishii, T., Igarashi, K., Katoh, Y., Oyake, T., Hayashi, N., Satoh, K., Hatayama, I., et al. 1997. An Nrf2/small Maf heterodimer mediates the induction of phase II detoxifying enzyme genes through antioxidant response elements. *Biochem. Biophys. Res. Commun.* **236**: 313–322.
- Itoh, K., Wakabayashi, N., Katoh, Y., Ishii, T., Igarashi, K., Engel, J.D., and Yamamoto, M. 1999. Keap1 represses nuclear activation of antioxidant responsive elements by Nrf2 through binding to the amino-terminal Neh2 domain. *Genes & Dev.* **13**: 76–86.
- Kelly, W.G., Xu, S., Montgomery, M.K., and Fire, A. 1997. Distinct requirements for somatic and germline expression of a generally expressed *Caenorhabditis elegans* gene. *Genetics* **146**: 227–238.
- Kenyon, C., Chang, J., Gensch, E., Rudner, A., and Tabtiang, R. 1993. A *C. elegans* mutant that lives twice as long as wild type. *Nature* **366**: 461–464.
- Kophengnavong, T., Carroll, A.S., and Blackwell, T.K. 1999. The SKN-1 amino terminal arm is a DNA specificity segment. *Mol. Cell Biol.* **19**: 3039–3050.
- Lee, R.Y., Hench, J., and Ruvkun, G. 2001. Regulation of *C. elegans* DAF-16 and its human ortholog FKHL1 by the *daf-2* insulin-like signaling pathway. *Curr. Biol.* **11**: 1950–1957.
- Lee, S.S., Kennedy, S., Tolonen, A.C., and Ruvkun, G. 2003. DAF-16 target genes that control *C. elegans* life-span and metabolism. *Science* **300**: 644–647.
- Lickert, H., Kutsch, S., Kanzler, B., Tamai, Y., Taketo, M.M., and Kemler, R. 2002. Formation of multiple hearts in mice following deletion of β -catenin in the embryonic endoderm. *Dev. Cell* **3**: 171–181.
- Maduro, M.F. and Rothman, J.H. 2002. Making worm guts: The gene regulatory network of the *Caenorhabditis elegans* endoderm. *Dev. Biol.* **246**: 68–85.
- Maduro, M.F., Meneghini, M.D., Bowerman, B., Broitman-Maduro, G., and Rothman, J.H. 2001. Restriction of mesoderm to a single blastomere by the combined action of SKN-1 and a GSK-3 β homolog is mediated by MED-1 and -2 in *C. elegans*. *Mol. Cell* **7**: 475–485.
- Mello, C.C., Kramer, J.M., Stinchcomb, D., and Ambros, V. 1991. Efficient gene transfer in *C. elegans*: Extrachromosomal maintenance and integration of transforming sequences. *EMBO J.* **10**: 3959–3970.
- Melov, S., Ravenscroft, J., Malik, S., Gill, M.S., Walker, D.W., Clayton, P.E., Wallace, D.C., Malfroy, B., Doctrow, S.R., and Lithgow, G.J. 2000. Extension of life-span with superoxide dismutase/catalase mimetics. *Science* **289**: 1567–1569.
- Nguyen, T., Sherratt, P.J., Huang, H.C., Yang, C.S., and Pickett, C.B. 2003. Increased protein stability as a mechanism that enhances Nrf2-mediated transcriptional activation of the antioxidant response element. Degradation of Nrf2 by the 26 S proteasome. *J. Biol. Chem.* **278**: 4536–4541.
- Ramos-Gomez, M., Kwak, M.K., Dolan, P.M., Itoh, K., Yamamoto, M., Talalay, P., and Kensler, T.W. 2001. Sensitivity to carcinogenesis is increased and chemoprotective efficacy of enzyme inducers is lost in *nrf2* transcription factor-deficient mice. *Proc. Natl. Acad. Sci.* **98**: 3410–3415.
- Reiter, J.F., Alexander, J., Rodaway, A., Yelon, D., Patient, R., Holder, N., and Stainier, D.Y. 1999. Gata5 is required for the development of the heart and endoderm in zebrafish. *Genes & Dev.* **13**: 2983–2995.
- Ren, P., Lim, C.S., Johnsen, R., Albert, P.S., Pilgrim, D., and Riddle, D.L. 1996. Control of *C. elegans* larval development by neuronal expression of a TGF- β homolog. *Science* **274**: 1389–1391.
- Rodaway, A. and Patient, R. 2001. Mesendoderm. An ancient germ layer? *Cell* **105**: 169–172.
- Schackwitz, W.S., Inoue, T., and Thomas, J.H. 1996. Chemosensory neurons function in parallel to mediate a pheromone response in *C. elegans*. *Neuron* **17**: 719–728.
- Sekhar, K.R., Yan, X.X., and Freeman, M.L. 2002. Nrf2 degradation by the ubiquitin proteasome pathway is inhibited by KIAA0132, the human homolog to INrf2. *Oncogene* **21**: 6829–6834.
- Shoichet, S.A., Malik, T.H., Rothman, J.H., and Shivdasani, R.A. 2000. Action of the *Caenorhabditis elegans* GATA factor END-1 in *Xenopus* suggests that similar mechanisms initiate endoderm development in ecdysozoa and vertebrates. *Proc. Natl. Acad. Sci.* **97**: 4076–4081.
- Stewart, D., Killeen, E., Naquin, R., Alam, S., and Alam, J. 2003. Degradation of transcription factor Nrf2 via the ubiquitin-proteasome pathway and stabilization by cadmium. *J. Biol. Chem.* **278**: 2396–2402.
- Talanian, R.V., McKnight, C.J., and Kim, P.S. 1990. Sequence-specific DNA binding by a short peptide dimer. *Science* **249**: 769–771.
- Thatcher, J.D., Fernandez, A.P., Beaster-Jones, L., Haun, C., and Okkema, P.G. 2001. The *Caenorhabditis elegans* *peb-1* gene encodes a novel DNA-binding protein involved in morphogenesis of the pharynx, vulva, and hindgut. *Dev. Biol.* **229**: 480–493.
- Thimmulappa, R.K., Mai, K.H., Srisuma, S., Kensler, T.W., Yamamoto, M., and Biswal, S. 2002. Identification of Nrf2-regulated genes induced by the chemopreventive agent sulforaphane by oligonucleotide microarray. *Cancer Res.* **62**: 5196–5203.
- Toone, W.M. and Jones, N. 1999. AP-1 transcription factors in yeast. *Curr. Opin. Genet. Dev.* **9**: 55–61.
- Toone, W.M., Morgan, B.A., and Jones, N. 2001. Redox control of AP-1-like factors in yeast and beyond. *Oncogene* **20**: 2336–2346.
- Walker, A.K., See, R., Batchelder, C., Kophengnavong, T., Groniger, J.T., Shi, Y., and Blackwell, T.K. 2000. A conserved transcription motif suggesting functional parallels between *C. elegans* SKN-1 and Cap 'n' Collar-related bZIP proteins. *J. Biol. Chem.* **275**: 22166–22171.
- Warga, R.M. and Nusslein-Volhard, C. 1999. Origin and development of the zebrafish endoderm. *Development* **126**: 827–838.
- Wolf, C.R. 2001. Chemoprevention: Increased potential to bear fruit. *Proc. Natl. Acad. Sci.* **98**: 2941–2943.